Overexpression of salusin-β downregulates adipoR1 expression to prevent fatty acid oxidation in HepG2 cells

AOHONG XU[1*], LEI WANG[1*], MIN LUO[1], HUAN ZHANG[1], MEIWEI NING[2], JINTONG PAN[1], XIUQUN DUAN[3], YUXUE WANG[1] and XIANG LIU[1]

[1]Department of Laboratory Medicine, Hubei University of Chinese Medicine, Wuhan, Hubei 430065; [2]Jiamusi College, Heilongjiang University of Chinese Medicine, Jiamusi, Heilongjiang 154007; [3]Clinical Laboratory, Ezhou Central Hospital, Ezhou, Hubei 436000, P.R. China

Received August 1, 2023; Accepted November 7, 2023

DOI: 10.3892/mmr.2023.13141

Abstract. Salusin-β and adiponectin receptor 1 (adipoR1) serve important roles in the development of certain cardiovascular diseases and lipid metabolism. However, to the best of our knowledge, the relationship between salusin-β and adipoR1, and their underlying mechanisms of action, currently remain unclear. In the present study, lentiviral vectors designed to overexpress salusin-β or knock down salusin-β expression were used in 293T and HepG2 cells. Semi-quantitative PCR was performed to investigate the relationship between salusin-β and adipoR1 mRNA expression in 293T cells. Western blotting was used to assess the protein expression levels of adipoR1, adenosine monophosphate-activated protein kinase (AMPK), acetyl-CoA carboxylase (ACC) and carnitine palmitoyl transferase 1A (CPT-1A) in transfected HepG2 cells. Simultaneously, HepG2 cells were treated with an adipoR1 inhibitor (thapsigargin) or agonist (AdipoRon) and the resultant changes in the expression levels of the aforementioned proteins were observed. Oil Red O staining and measurements of cellular triglyceride levels were performed to assess the extent of lipid accumulation in HepG2 cells. The results demonstrated that salusin-β overexpression downregulated adipoR1 expression and inhibited the phosphorylation of AMPK and ACC, which led to decreased CPT-1A protein expression. By contrast, salusin-β knockdown increased adipoR1 expression and promoted the phosphorylation of AMPK and ACC, which conversely enhanced CPT-1A protein expression. Treatment with adipoR1 agonist, AdipoRon, reversed the effects of salusin-β overexpression. In addition, salusin-β overexpression enhanced intracellular lipid accumulation in HepG2 cells induced by free fatty acid treatment. These findings highlighted the potential regulatory role of salusin-β in adipoR1-mediated signaling pathways. To conclude, the present study provided insights into the regulation of fatty acid metabolism by the liver. In particular, salusin-β may serve as a potential target for the therapeutic intervention of metabolic disorders of lipids.

Correspondence to: Dr Xiuqun Duan, Clinical Laboratory, Ezhou Central Hospital, 9 Wenxin Road, Ezhou, Hubei 436000, P.R. China
E-mail: 1529784391@qq.com

Professor Xiang Liu, Department of Laboratory Medicine, Hubei University of Chinese Medicine, 16 Huangjiahu West Road, Baishazhou Avenue, Hongshan, Wuhan, Hubei 430065, P.R. China
E-mail: lx1568@hbtcm.edu.cn

*Contributed equally

Key words: salusin-β, adiponectin receptor 1, adenosine monophosphate-activated protein kinase, fatty acid oxidation, lipid deposition

Introduction

Salusin-β is a 20-amino acid bioactive peptide encoded by the human torsion dystonia gene torsin family 2 member A (TOR2A). The TOR2A gene undergoes selective splicing and translation within the cell, which results in the formation of a 242-amino acid residue, preprosalusin (1,2). Cleavage of the N-terminal portion of preprosalusin produces prosalusin, which then undergoes further cleavage of the signal peptide to produce the active salusin-β peptide molecule (1). Salusin-β is expressed in the neuroendocrine system, monocytes and macrophages (2). It has previously been reported that salusin-β serves a regulatory role in various physiological processes, including blood pressure regulation, heart rate modulation, intracellular signaling, promotion of mitosis and proinflammatory factor expression (3-5). Notably, salusin-β has been implicated in the pathogenesis of atherosclerosis, a cardiovascular disease characterized by arterial plaque formation (6). Aydin and Aydin (7) employed Pearson correlation analysis and reported that, in a rat model of lipid metabolism syndrome, serum concentrations of salusin-β and high-density lipoprotein (HDL) cholesterol were found to be decreased compared with those in the control group, while glucose and triglyceride (TG) levels were increased. These findings suggested a potential association between salusin-β and lipid metabolism in the context of lipid metabolism syndrome. Additionally, Chen and Jin (8) reported that a reduction in salusin-β inhibits cellular lipid accumulation and reduces cholesterol levels. However, the precise mechanism

by which salusin-β can regulate lipid metabolism remains to be fully elucidated.

Adiponectin receptor 1 (adipoR1) is a pivotal component of adipokine signaling and is responsible for mediating the physiological effects of adiponectin. AdipoR1 has seven transmembrane domains (9). However, different from other types of G protein-coupled receptors (GPCRs), the N-terminus can bind intracellular adaptive proteins, whereas the C-terminus binds to extracellular adiponectin (9). AdipoR1 activation by binding to adiponectin triggers various downstream signaling pathways that can regulate lipid metabolism. In particular, adipoR1 is predominantly expressed in skeletal muscle and can activate adenosine monophosphate-activated protein kinase (AMPK), which phosphorylates acetyl-CoA carboxylase (ACC). ACC serves an important role in the regulation of carnitine palmitoyl transferase 1A (CPT-1A), an enzyme involved in mitochondrial fatty acid β-oxidation (9,10). Impaired fatty acid β-oxidation contributes to dyslipidemia (10). Therefore, adipoR1 is an important protein involved in the regulation of lipid metabolism.

Based on the aforementioned biological functions of salusin-β and adipoR1 and their opposing biological effects on lipid metabolism, in addition to our pilot study showing an association between the expression levels of salusin-β and adipoR1, a hypothesis that salusin-β can regulate fatty acid oxidation via adipoR1 in HepG2 cells was proposed. The present study aimed to explore the potential association and molecular mechanisms of salusin-β and adipoR1 in lipid metabolism by manipulating salusin-β expression using lentiviral vectors *in vitro*, to provide valuable insights into the pathogenesis of dyslipidaemia and to identify potential therapeutic targets.

Materials and methods

Materials and reagents. Premix Taq™ DNA Polymerase (cat. no. RR003A), T4 DNA Ligase (cat. no. 2011A), *Xho*I (cat. no. 1094A) and *Bam*HI (cat. no. 1010A) were purchased from Takara Bio, Inc. *Age*I (cat. no. R3552) and *Eco*RI (cat. no. R3101) were purchased from New England BioLabs, Inc. Anti-salusin-β antibodies (cat. no. PAC026Hu08) were purchased from Wuhan USCN Business Co., Ltd. Anti-adipoR1 (cat. no. ab70362), anti-CPT-1A (cat. no. ab234111) and anti-GAPDH (cat. no. ab185059) antibodies were purchased from Abcam. Anti-AMPK (cat. no. 5831), anti-phosphorylated (p-)AMPK (cat. no. 2535), anti-ACC (cat. no. 3676) and anti-p-ACC (cat. no. 11818) antibodies were purchased from Cell Signaling Technology, Inc. HRP-labelled goat anti-rabbit IgG antibodies (cat. no. E-AB-1102) and the BCA Protein Colorimetric Assay Kit (cat. no. E-BC-K318-M) were purchased from Elabscience Biotechnology, Inc. Stock solutions of 10 mM oleic acid (OA; Shanghai Macklin Biochemical Co., Ltd.) and 20 mM palmitic acid (PA; Shanghai Macklin Biochemical Co., Ltd.) prepared in 10% fatty acid-free BSA (Sigma-Aldrich; Merck KGaA) were diluted in the high-glucose DMEM (Procell Life Science & Technology Co., Ltd.) medium to obtain the desired final concentration of free fatty acids (FFAs) mixture (OA/PA molar ratio, 2:1). Oil Red O stock solution (0.5%; Beijing Solarbio Science & Technology Co., Ltd.) was prepared with isopropanol alcohol. The TG assay kit (cat. no. A110-1-1) was purchased from Nanjing Jiancheng Bioengineering Institute.

Construction of recombinant plasmids. Based on the human TOR2A gene sequence from the National Center for Biotechnology Information (NCBI) gene library (NM_001134430.3) (https://www.ncbi.nlm.nih.gov/nuccore/NM_001134430.3), the nucleotide sequence of salusin-β encoded by bases 598-657 was determined. Primers containing restriction enzyme sites and protective bases were designed to target salusin-β and the specificity of the sequence was confirmed through Basic Local Alignment Search Tool (BLAST) analysis in the NCBI database (https://www.ncbi.nlm.nih.gov/tools/primer-blast/index.cgi?LINK_LOC=BlastHome). The primers used were as follows: Salusin-β forward, 5'-CGCGGATCCGCCATCTTC ATCTTCATCAG-3' (the *Bam*HI enzyme restriction site is underlined) and reverse, 5'-CCGCTCGAGAGGAGGCGC TCTTCC-3' (the *Xho*I enzyme restriction site is underlined). Considering the potential off-target effects and poor interference efficiency of short hairpin RNA (shRNA/sh), three pairs of shRNA sequences targeting salusin-β were designed using the BLOCK-iT™ RNAi Designer (Thermo Fisher Scientific, Inc.), and referred to as sh-Salusin-β_1, sh-Salusin-β_2 and sh-Salusin-β_3 (Table I). The sequence structure of the shRNA sense strand was as follows: 5'-'CCGG' (hanging end for *Age*I restriction enzyme), salusin-β target sequence (21 bp), 'CTCGAG' (loop), reverse complement of the target sequence and 'TTTTTG' (transcription termination sequence for RNA polymerase III)-3'. The antisense strand sequence of the shRNA was complementary to the sense strand, while the 5'-'AATT' sequence served as the hanging end for the *Eco*RI restriction enzyme. Single-stranded salusin-β nucleotides, primers and shRNA were then synthesized. Lentivirus vectors pHAGE (cat. no. 118692; Addgene, Inc.) and pLKO.1 (cat. no. 8453; Addgene, Inc.), envelope plasmids psPAX2 (cat. no. 12260; Addgene, Inc.) and pMD2G (cat. no. 12259; Addgene, Inc.), the pLKO.1-sh-Mock plasmid (containing a non-mammalian targeting shRNA sequence 5'-CCGGCAACAAGATGAAGA GCACCAACTCGAGTTGGTGCTCTTCATCTTGTTGTTT TTG-3'; cat. no. SHC002; Sigma-Aldrich; Merck KGaA) and Top10 competent cells (cat. no. B528412; Sangon Biotech Co., Ltd.) were donated by the Basic Medicine Laboratory at Wuhan Huazhong University of Science and Technology (Wuhan, China). The single-stranded nucleotides of salusin-β synthesized by Sangon Biotech Co., Ltd. were added to a PCR reaction system containing Premix Taq™ DNA Polymerase (Takara Bio, Inc.) and amplified with the primers containing restriction sites (Table II); the thermocycling conditions, agarose gel and visualization methods are described in the subsequent s-qPCR section. The PCR products were then purified according to the manufacturer's instructions of the TaKaRa MiniBEST Agarose Gel DNA Extraction Kit Ver.4.0 (cat. no. 9762; Takara Bio, Inc.), and incubated with *Bam*HI at 30˚C for 3 h, followed by digestion with *Xho*I at 37˚C for 3 h. The resulting salusin-β DNA fragments were ligated into the pHAGE vector at a molar ratio between 3:1 and 10:1 using T4 DNA ligase (11,12). The double-stranded shRNA nucleotides were obtained through the annealing of sense and antisense strands before being ligated

Table I. Salusin-β-specific shRNA sequences.

shRNA	Sequence (5'-3')
sh-Salusin-β_1	Sense: CCGGGCCATCTTCATCTTCATCAGACTCGAGTCTGATGAAGATGAAGATGGCTTTTTG Antisense: AATTCAAAAAGCCATCTTCATCTTCATCAGACTCGAGTCTGATGAAGATGAAGATGGC
sh-Salusin-β_2	Sense: CCGGGGCTTCTCAAACTCGGGCATCCTCGAGGATGCCCGAGTTTGAGAAGCCTTTTTG Antisense:AATTCAAAAAGGCTTCTCAAACTCGGGCATCCTCGAGGATGCCCGAGTTTGAGAAGCC
sh-Salusin-β_3	Sense: CCGGGCTTCTCAAACTCGGGCATCACTCGAGTGATGCCCGAGTTTGAGAAGCTTTTTG Antisense:AATTCAAAAAGCTTCTCAAACTCGGGCATCACTCGAGTGATGCCCGAGTTTGAGAAGC

sh/shRNA, short hairpin RNA.

Table II. Primers used for PCR analysis.

Gene target	Sequence (5'-3')
WPRE	F: CGCTATGTGGATACGCTGCTTTA R: GCAACCAGGATTTATACAAGGAGGA
sh-Salusin-β_1	F: CGAGACTAGCCTCGAGCGGCC R: AAGATGAAGATGGCCCGGTGTTTCGT
sh-Salusin-β_2	F: CGAGACTAGCCTCGAGCGGCC R: CTCGAGGATGCCCGAGTTTGAGAAGC
sh-Salusin-β_3	F: CGAGACTAGCCTCGAGCGGCC R: CGAGTGATGCCCGAGTTTGAGAAGCC
Salusin-β	F: CGCGGATCCGCCATCTTCATCTTCATC AG R: CCGCTCGAGAGGAGGCGCTCTTCC
AdipoR1	F: ACGGTGGAACTGGCTGAAC R: CCATGTAGCAGATAGTCGTTGTC
GAPDH	F: GTCTCCTCTGACTTCAACAGCG R: ACCACCCTGTTGCTGTAGCCAA

AdipoR1, adiponectin receptor 1; F, forward; R, reverse; sh, short hairpin RNA; WPRE, woodchuck hepatitis virus post-transcriptional regulatory element.

into the pLKO.1 vector using *Age*I and *Eco*RI restriction sites at 37˚C for 15 min. After 12 h ligation at 16˚C, the products were added to 100 μl Top10 competent cells, mixed gently, and placed on ice for 30 min, followed by a 90 sec incubation at 42˚C in a water bath and rapidly returned to ice for 2 min. Subsequently, 800 μl LB liquid medium (Biosharp Life Sciences) was added, and the mixture was shaken at 25 x g at 37˚C for 1 h. Then, 200 μl bacterial culture was evenly spread on LB agar plates containing ampicillin (100 μg/ml) and incubated for 16 h at 37˚C in the inverted position. Monoclonal bacterial colonies were then randomly selected as PCR templates, with the forward and reverse primer sequences listed in Table II, and amplified using Premix Taq™ DNA Polymerase (Takara Bio, Inc; the thermocycling conditions, agarose gel and visualization methods are described in the subsequent s-qPCR section). The recombinant plasmids were confirmed through Sanger sequencing, followed by large-scale plasmid extraction using the SanPrep Column Plasmid Mini-Preps Kit (cat. no. B518191; Sangon Biotech Co., Ltd.), for subsequent experiments.

Cell culture and lentivirus packaging. 293T cells (cat. no. CRL-3216TM; American Type Culture Collection) were obtained from Wuhan Huazhong University of Science and Technology (Wuhan, China). The HepG2 liver cancer cell line (cat. no. ECL-0103) was purchased from Enova (Wuhan) Biotechnology Co., Ltd. and authenticated by short tandem repeat analysis. Cells were cultured in complete medium composed of high-glucose DMEM (Procell Life Science & Technology Co., Ltd.) supplemented with 10% FBS (Invitrogen; Thermo Fisher Scientific, Inc.) and 1% penicillin/streptomycin at 37˚C in a humidified atmosphere of 5% CO_2. Cells at passages 10-15 were used for experiments and the medium was refreshed every 48-72 h.

For lentivirus packaging using a second-generation transduction system, when the cell confluence reached 50-60%, 293T cells were transfected with 4 μg constructed recombinant plasmid (pHAGE-Salusin-β or pLKO.1-sh-Salusin-β) or the corresponding blank vector plasmid (pHAGE or pLKO.1-sh-Mock), along with 3 μg psPAX2 and 1 μg pMD2.G packaging plasmids (mass ratio of the three plasmids, 4:3:1). Transfection was performed at 37˚C using the Simple-fect reagent (Signaling Dawn Biotech) following the manufacturer's instructions. After 24 h, the medium was replaced with fresh medium. Cell supernatants were collected at 48 and 72 h and centrifuged at 800 x g for 10 min at 4˚C, then filtered through a 0.45-μm filter to obtain the viral suspension. The viral suspension was sorted into 1.5-ml Eppendorf tubes (Eppendorf SE; 1 ml/tube), and stored at -80˚C. To verify the presence of the target gene, primers were designed for the woodchuck hepatitis virus post-transcriptional regulatory element (WPRE) gene on the pHAGE vector (Table II). This gene is not found in humans and the specificity of the primers was confirmed by conducting a BLAST analysis in the NCBI RNA virus gene database (https://www.ncbi.nlm.nih.gov/tools/primer-blast/primertool.cgi?ctg_time=1699883569&job_key=KSP3XoH-jFarbBxpEQk4W2sSKWlGATJ0Rw&CheckStatus=Check). Additionally, a forward primer was designed for the U6 promoter in the pLKO.1-sh-Salusin-β recombinant interference vector and different reverse primers were designed for the three different shRNA sequences targeting salusin-β. RNA was extracted from the viral suspension and PCR was performed to amplify the specific fragments of WPRE and sh-Salusin-β.

The successful viral synthesis was initially detected by 1.5% agarose gel electrophoresis and subsequently verified by Sanger sequencing. The sequencing results and BLAST analysis of WPRE PCR products are shown in Fig. S1. The specific PCR products of sh-Salusin-β_{1-3} were sequenced and then aligned with the sequence of recombinant plasmid pLKO.1-sh-Salusin-β_{1-3} using SnapGene v6.0.2 software (GSL Biotech LLC; Figs. S2-S4).

Preparation of transmission electron microscopy (TEM) specimens. After collecting the supernatant of lentivirus packaging, 3 ml pre-cooled 2.5% glutaraldehyde (Shanghai Macklin Biochemical Co., Ltd.) was added to 293T cells (confluence, ~100%) in a 10-cm dish. Cells were fixed for 1 h at room temperature, then scraped off from the dish and centrifuged at 600 x g for 5 min at 4˚C to obtain cell pellets. Cells were resuspended in ~1 ml of supernatant, then transferred to a 1.5-ml Eppendorf tube. Cells were allowed to settle vertically for 1 h at room temperature before the supernatant was discarded and 1 ml pre-cooled 2.5% glutaraldehyde was added. Samples were fixed overnight for 16 h at 4˚C. Subsequently, the samples were transported to the Electron Microscopy Room at Wuhan University People's Hospital (Wuhan, China) for further processing. Samples were washed thrice with PBS for 10 min, then fixed using 1% osmium tetroxide at 4˚C for 1 h. After three additional rinses with PBS, the samples were dehydrated using an ascending ethanol series (50, 70, 90, 95, 100, 100 and 100%). Following infiltration and embedding in epoxy resin at 60˚C for 24 h, the samples were sliced into 50-nm sections using a microtome. The resulting sections were then stained with uranyl acetate for 30 min and lead citrate for 15 min at room temperature. Finally, the lentivirus morphology was observed using the JEM-1230 transmission electron microscope (JEOL, Ltd.).

Measurement of lentiviral titer and MOI. 293T cells ($1x10^5$ cells/well) were seeded into 6-well plates and supplemented with 0, 5, 10, 15, 20 or 30 μl modified virus and complete medium containing 8 μg/ml polybrene (Biosharp Life Sciences) to a volume of 2 ml. After 24 h of incubation at 37˚C, the medium was replaced with fresh complete medium. On day 3, cells were digested with 0.25% trypsin at 37˚C for 5 min and the resulting cell suspension from each well was divided into two equal parts and seeded into 6-well plates. On day 4, the medium was replaced with either complete medium containing 2 μg/ml puromycin or fresh complete medium as a control. Cell viability was observed using a light inverted microscope to see if the cells were floating. Floating cells indicate that the cells are dead. When cells in the control puromycin-treated group died, trypan blue (cat. no. C0040; Beijing Solarbio Science & Technology Co., Ltd.) was used to stain the 293T cells at 37˚C for 3 min and live cell counting were performed on the treated cells through a light microscope (Olympus Corporation). The 'number of live cells' was calculated for the puromycin-treated cells, whereas the 'number of control cells' was calculated for control cells. The titer of each viral dose group was then calculated according to the following formula: Titer (TU/ml)=(number of live cells x number of initial cells)/(number of control cells x virus volume) and the mean of the six viral dose groups was taken to obtain the final viral titer.

Based on the reference range of the MOI for lentivirus-infected 293T cells being 1-3 (13), MOIs of 0, 1, 2, 3, 4 and 5 were used to screen the optimal MOI values for subsequent experiments. 293T cells were seeded ($8x10^5$ cells/well) into 6-well plates and when the cell density reached 80% on day 2 (~$2x10^6$ cells) at 37˚C for 24 h, an appropriate volume of virus was added for infection [volume of virus added/well (μl)=(MOI x number of cells/titer) x1,000]. After incubation at 37˚C for 24 h, fresh medium containing 2 μg/ml puromycin was added to the cells for selection. Following further incubation at 37˚C for 3-5 days, when floating clumps of dead cells appeared, the corresponding minimum MOI value was considered to be the optimal MOI for 293T cells.

Transient cell transfection and FFA-induced steatosis of HepG2 cells. HepG2 or 293T cells were seeded ($1x10^5$ cells/well) in 6-well plates 1 day prior to transfection. When the cell density reached 60-70%, a mixture containing 1 ml modified virus (pHAGE, pHAGE-Salusin-β, pLKO.1-sh-Mock or pLKO.1-sh-Salusin-β) suspension, 840 μl medium and 160 μl polybrene (final concentration, 8 μg/ml) was added to the cells. The control group was treated without the virus suspension. After incubation at 37˚C for 24 h, RNA and proteins were immediately isolated from the cells for gene expression analysis using semi-quantitative PCR (s-qPCR) and protein expression analysis using western blotting (WB).

To investigate the mechanism of the regulatory effect of salusin-β on the AMPK/ACC/CPT-1A signaling pathway via adipoR1, HepG2 cells were first infected with modified lentivirus (pHAGE, pHAGE-Salusin-β, pLKO.1-sh-Mock or pLKO.1-sh-Salusin-β) at 37˚C for 24 h. Subsequently, the cells were treated with either an adipoR1 agonist (10 μM AdipoRon; Selleck Chemicals) or an adipoR1 inhibitor (1 μM thapsigargin; Sigma-Aldrich; Merck KGaA) at 37˚C for 24 h, before the protein expression levels of downstream molecules were evaluated.

To assess the impact of salusin-β on lipid metabolism, transiently-transfected HepG2 cells were incubated with 200 μM FFAs to induce lipid accumulation at 37˚C for 24 h. The control group was treated at 37˚C for 24 h with the same volume of 10% BSA solution as the FFA-treated groups.

S-qPCR. Total RNA was extracted from the cells using RNAiso Plus reagent (Takara Bio, Inc.) and quantified using a Nano400 analyzer (Hangzhou Allsheng Instruments Co., Ltd.). RNA was diluted to a concentration of 500 ng/μl and reverse transcribed into cDNA using Reverse Transcriptase XL (AMV) (Takara Bio, Inc.) according to the manufacturer's protocol. A preliminary gradient cycle number PCR experiment determined that 30 cycles were optimal for the exponential amplification of the salusin-β and adipoR1 genes. According to the manufacturer's instructions, Premix Taq™ DNA Polymerase was used to separately amplify the target gene and internal reference gene (GAPDH) in different tubes from the same batch. The following thermocycling conditions were used for PCR: Initial denaturation at 95˚C for 3 min; 30 cycles of 94˚C for 30 sec, 64˚C for salusin-β/60˚C for adipoR1 and GAPDH for 30 sec and 72˚C for 30 sec; and a final extension at 72˚C for 5 min. After amplification, the PCR products were electrophoresed on a 2% agarose gel containing the nucleic acid stain

SuperRed/GelRed (cat. no. BS354B; Biosharp Life Sciences) in Tris-acetate-EDTA buffer with a constant voltage of 120 V. Subsequently, the gel was visualized using the Tanon-1600 Gel Imaging System (Tanon Science and Technology Co., Ltd.). The cumulative optical density values were measured using the ImageJ software (version 1.52a; National Institutes of Health), before the expression of the target gene was normalized to that of GAPDH as the internal reference gene for relative quantification. The primer sequences used for PCR amplification are provided in Table II. All PCR amplification products in the present study were verified by sequencing and BLAST analysis (Figs. S5-S7).

WB. WB was performed to assess the protein levels of salusin-β, adipoR1, CPT-1A, p-AMPK and p-ACC in 293T and HepG2 cells. Total protein was extracted from cells using RIPA lysis buffer (Dalian Meilun Biology Technology Co., Ltd.) supplemented with 1X PMSF protease inhibitor and 1X phosphatase inhibitor. Protein concentrations were determined using a BCA protein quantification kit. Samples were mixed with 5X SDS loading buffer and heated at 95˚C for 10 min. Each lane was loaded with 20 μg protein and proteins were separated by 10% SDS-PAGE. Proteins were transferred onto a PVDF membrane. The membrane was blocked with 5% skimmed milk powder at room temperature for 1 h, washed with Tris-buffered saline-0.1% Tween-20 (TBST) and incubated overnight for 14 h at 4˚C with primary anti-salusin-β (1:500), anti-adipoR1 (1:1,000), anti-AMPK (1:1,000), anti-p-AMPK (1:1,000), anti-ACC (1:1,000), anti-p-ACC (1:1,000), anti-CPT-1A (1:1,000) and anti-GAPDH (1:5,000) antibodies. After washing with TBST, the membrane was incubated with an HRP-conjugated secondary antibodies (1:2,000) at room temperature for 1 h, followed by additional washing. Meilunbio® FGSuper Sensitive ECL Luminescence Reagent (Dalian Meilun Biology Technology Co., Ltd.) was used for protein band visualization. GAPDH was used as the internal reference. Measurements of the protein band grayscale values were performed using ImageJ software (version 1.52a; National Institutes of Health). The relative protein expression levels were calculated as the ratio of the gray value of the target band to the gray value of the internal reference protein band. The phosphorylation levels of AMPK and ACC were determined by calculating the ratio of p-AMPK (Thr172)/AMPK and p-ACC (Ser79)/ACC, respectively.

Oil Red O staining. Oil Red O staining was performed to assess intracellular lipid droplet levels. HepG2 cells (1x10^5 cells/well) were seeded in 6-well plates at 37˚C for 24 h, washed with PBS, fixed with 4% paraformaldehyde at room temperature for 15 min and then washed twice with PBS. Cells were incubated with 60% isopropanol alcohol for 1 min, followed by staining with fresh Oil Red O working solution (oil red O dye storage solution/ddH_2O ratio, 3:2) for 20 min at room temperature. After staining, the cells were washed with 60% isopropanol alcohol for 30 sec, treated with 10% hematoxylin at room temperature for 2 min and then washed with PBS to remove excess dye. The stained HepG2 cells were imaged using a light Olympus microscope (Olympus Corporation). ImageJ software was utilized to analyze the staining area in the images and quantify the intracellular lipid content.

TG assay. HepG2 cells (1x10^5 cells/well) were seeded in 6-well plates and incubated at 37˚C for 24 h. After infection with lentivirus at 37˚C for 24 h, the cells were further incubated with 200 μM FFAs at 37˚C for 24 h. Subsequently, the cells were treated with RIPA lysis buffer at 4˚C for 30 min, followed by centrifugation at 10,000 x g for 10 min at 4˚C to collect the lysate. Cellular intracellular TG levels were then determined using a commercial kit according to the manufacturer's instructions. Protein quantification was performed using the BCA method. Intracellular lipid deposition was assessed by calculating the TG/protein content.

Statistical analysis. All data were analyzed using GraphPad Prism software (version 8.0; Dotmatics). Each experiment was performed with three replicates, and the mean value was used for subsequent analysis. One-way ANOVA followed by Tukey's test was used to analyze statistically significant differences among multiple groups. All measurement data are presented as the mean ± standard error of the mean. $P<0.05$ was considered to indicate a statistically significant difference.

Results

Construction and identification of the recombinant pHAGE-Salusin-β and pLKO.1-sh-Salusin-β plasmids. A recombinant pHAGE-Salusin-β plasmid and three recombinant pLKO.1-sh-Salusin-β plasmids were successfully constructed (Fig. 1A). Monoclonal colony PCR results were analyzed using agarose gel electrophoresis (Fig. 1B). The PCR product from the pHAGE-Salusin-β monoclonal clone (78 bp) appeared as a band at ~100 bp. By contrast, the amplified products of sh-Salusin-β_1, sh-Salusin-β_2 and sh-Salusin-β_3 (298, 311 and 309 bp, respectively) corresponded to bands at ~300 bp, consistent with the expected sizes of the amplified sequences. Sequencing analysis confirmed an identical match with the original sequences (Fig. 1C), which indicated the successful construction of the recombinant pHAGE-Salusin-β overexpression plasmid and the three recombinant pLKO.1-sh-Salusin-β interference plasmids.

Construction and validation of lentiviral vectors for salusin-β interference in 293T cells. 293T cells were separately transfected with recombinant pHAGE-Salusin-β and pLKO.1-sh-Salusin-β plasmids, along with psPAX2 and pMD2.G packaging plasmids, and the viral suspension was collected from the cell supernatant at 48 and 72 h (Fig. 2A). On day 4, microscopic analysis of the transfected cells demonstrated distinct cellular changes, including small lesions, floating granules and cell fusion (Fig. 2B). TEM confirmed the presence of spherical virus particles in the cytoplasm of the transfected cells, which suggested successful packaging and synthesis of lentiviral particles (Fig. 2C). Subsequently, the harvested viruses were subjected to PCR analysis, and the results confirmed the presence of a specific fragment of 98 bp corresponding to WPRE in the pHAGE and pHAGE-Salusin-β construct, as well as the specific PCR products for sh-Salusin-β1 (298 bp), sh-Salusin-β2 (311 bp) and sh-Salusin-β3 (309 bp) in the pLKO.1-sh-Salusin-β_{1-3} constructs (Fig. 2D). These findings confirmed the successful introduction of lentiviral vectors

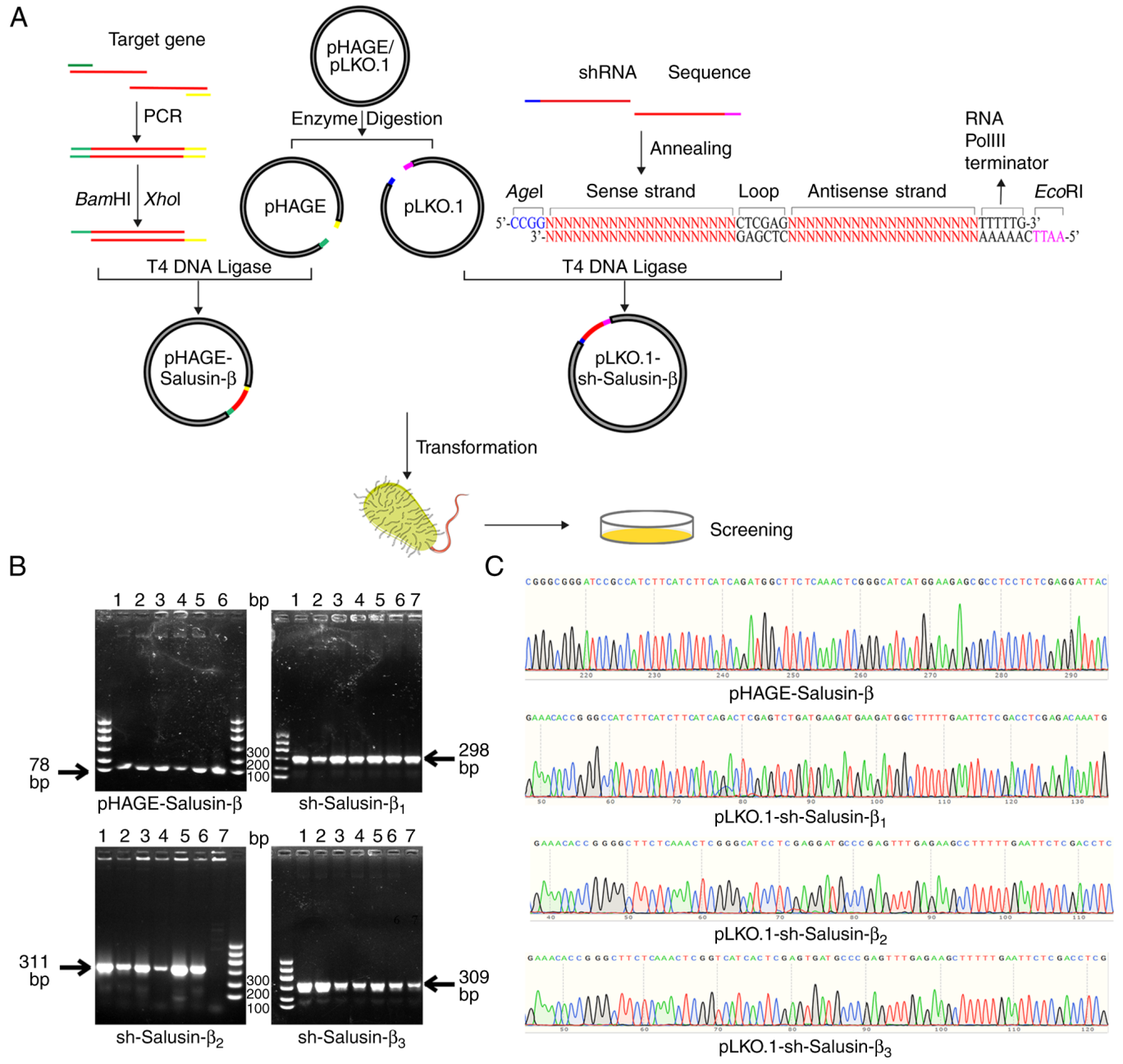

Figure 1. Construction and identification of recombinant plasmids. (A) Schematic diagram of the construction of recombinant plasmids pHAGE-Salusin-β and pLKO.1-sh-Salusin-β. (B) Identification of recombinant plasmids pHAGE-Salusin-β and pLKO.1-sh-Salusin-β by agarose gel electrophoresis of the PCR products of the colonies. Each lane number represents a different monoclonal colony of PCR product from each recombinant plasmid. (C) DNA sequencing peak plots of recombinant plasmids. pHAGE and pLKO.1 are lentiviral expression vectors; pHAGE-Salusin-β is the Salusin-β overexpression recombinant plasmid; pLKO.1-sh-Salusin-$\beta_{1\text{-}3}$ and sh-Salusin-$\beta_{1\text{-}3}$ are the Salusin-β interference recombinant plasmids. sh/shRNA, short hairpin RNA.

into 293T cells and the production of functional lentiviral particles.

Following the transfection of 293T cells with the lentiviral constructs for 24 h, the mRNA expression levels of salusin-β were evaluated using s-qPCR. Nucleic acid electrophoresis demonstrated a noticeable decrease in the signal intensity of the target bands (78 bp) in the three groups of cells expressing pLKO.1-sh-Salusin-β (Fig. 2E). Compared with those in the sh-Mock group treated with lentivirus containing a nonsense shRNA, the relative expression levels of salusin-β mRNA were significantly reduced in the sh-Salusin-β_1, sh-Salusin-β_2 and sh-Salusin-β_3 groups, with the sh-Salusin-β_2 group exhibiting the most pronounced decrease (Fig. 2F). By contrast, no significant difference in relative salusin-β mRNA expression was observed between the sh-Mock group and the control group without lentiviral treatment. These results confirmed the successful knockdown of salusin-β mRNA expression by the three recombinant pLKO.1-sh-Salusin-β vectors in 293T cells, with sh-Salusin-β_2 exhibiting the strongest effect. Consequently, pLKO.1-sh-Salusin-β2 was selected as the optimal recombinant vector for subsequent experiments.

Salusin-β expression negatively regulates adipoR1 expression in 293T cells. To explore the association between salusin-β and

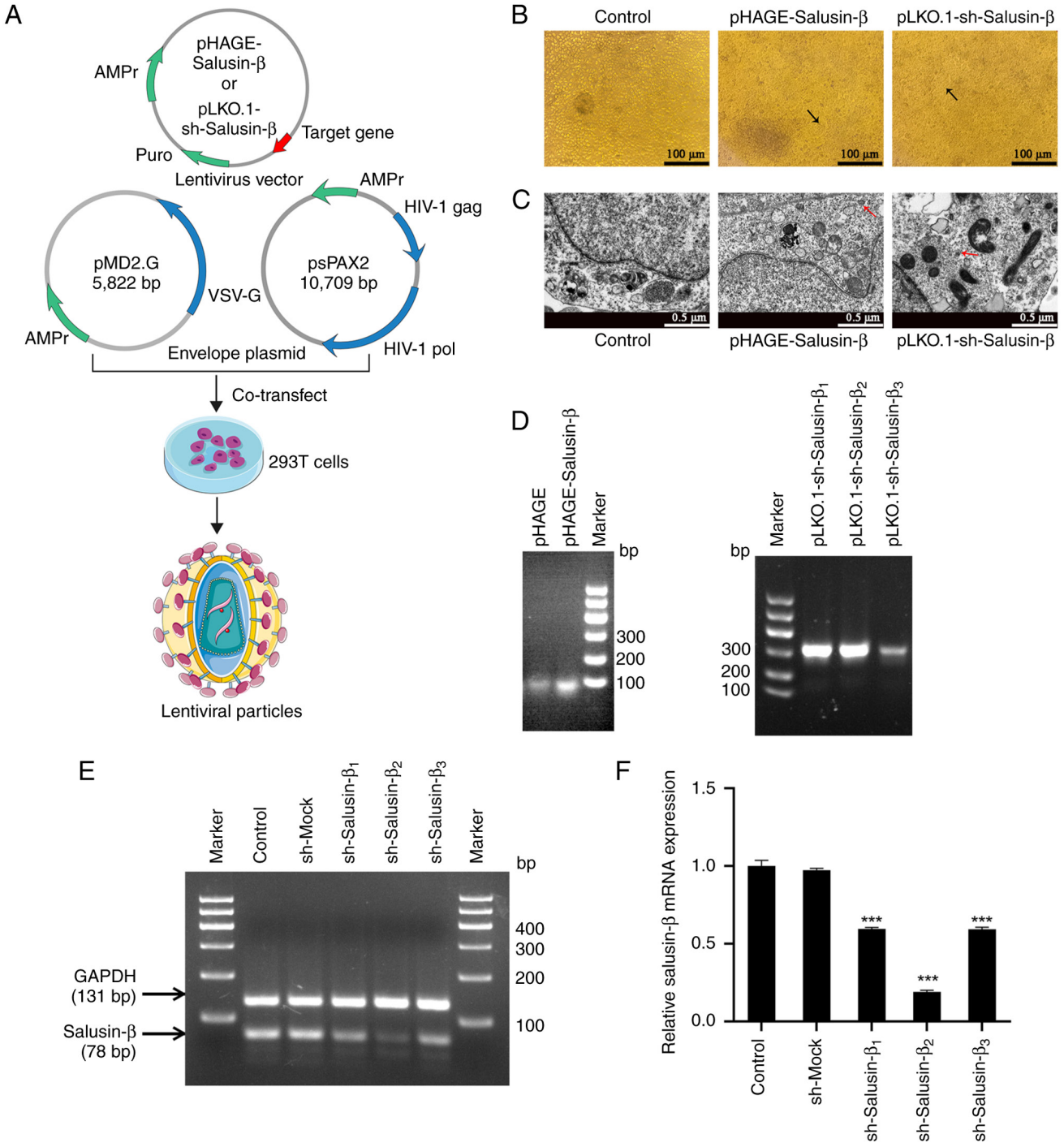

Figure 2. Packaging and identification of the recombinant lentiviruses. (A) Schematic representation of the process used for lentivirus synthesis. (B) Representative images of the cytopathic effect in 293T cells. On day 4 of lentivirus packaging, small lesions appeared in the corresponding plasmid-transfected groups, whereby the transfected cells fused to form syncytia (indicated by black arrows). Scale bar, 100 μm. (C) Transmission electron microscopy images of 293T cells transfected with recombinant lentiviral vectors and control cells. Red arrows indicate lentiviral particles. Scale bar, 0.5 μm. (D) Gel electrophoresis of PCR target gene products from the lentiviral particles harvested from the 293T cell culture medium. (E) Gel electrophoresis and semi-quantitative PCR of salusin-β mRNA from 293T cells after lentivirus-mediated transduction of the shRNA against salusin-β or a sequence without a hairpin structure for 24 h. (F) Relative mRNA expression levels of salusin-β in the different groups of transfected 293T cells. Data are presented as the mean ± standard error of the mean (n=3). ***P<0.001 vs. sh-Mock group. Control, negative control group without lentiviral treatment; pHAGE, empty lentiviral treatment group used as a control for pHAGE-Salusin-β; sh-Mock, lentiviral treatment group containing a non-targeting shRNA sequence as a control for sh-Salusin-β; pHAGE-Salusin-β, lentiviral treatment group for overexpression of Salusin-β; pLKO.1-sh-Salusin-$\beta_{1\text{-}3}$ and sh-Salusin-$\beta_{1\text{-}3}$, lentiviral treatment group for interference of Salusin-β. sh/shRNA, short hairpin RNA; puro, puromycin resistance; AMPr, ampicillin resistance; HIV-1, human immunodeficiency virus type 1; pol, polymerase; VSV-G, vesicular stomatitis virus G.

the lipid metabolism-related protein adipoR1, 293T cells were divided into control and treatment groups before undergoing transient lentivirus transfection. S-qPCR results demonstrated that salusin-β mRNA expression was altered depending on whether cells were transfected with the salusin-β overexpression plasmid or shRNA plasmids (Fig. 3A and B). There

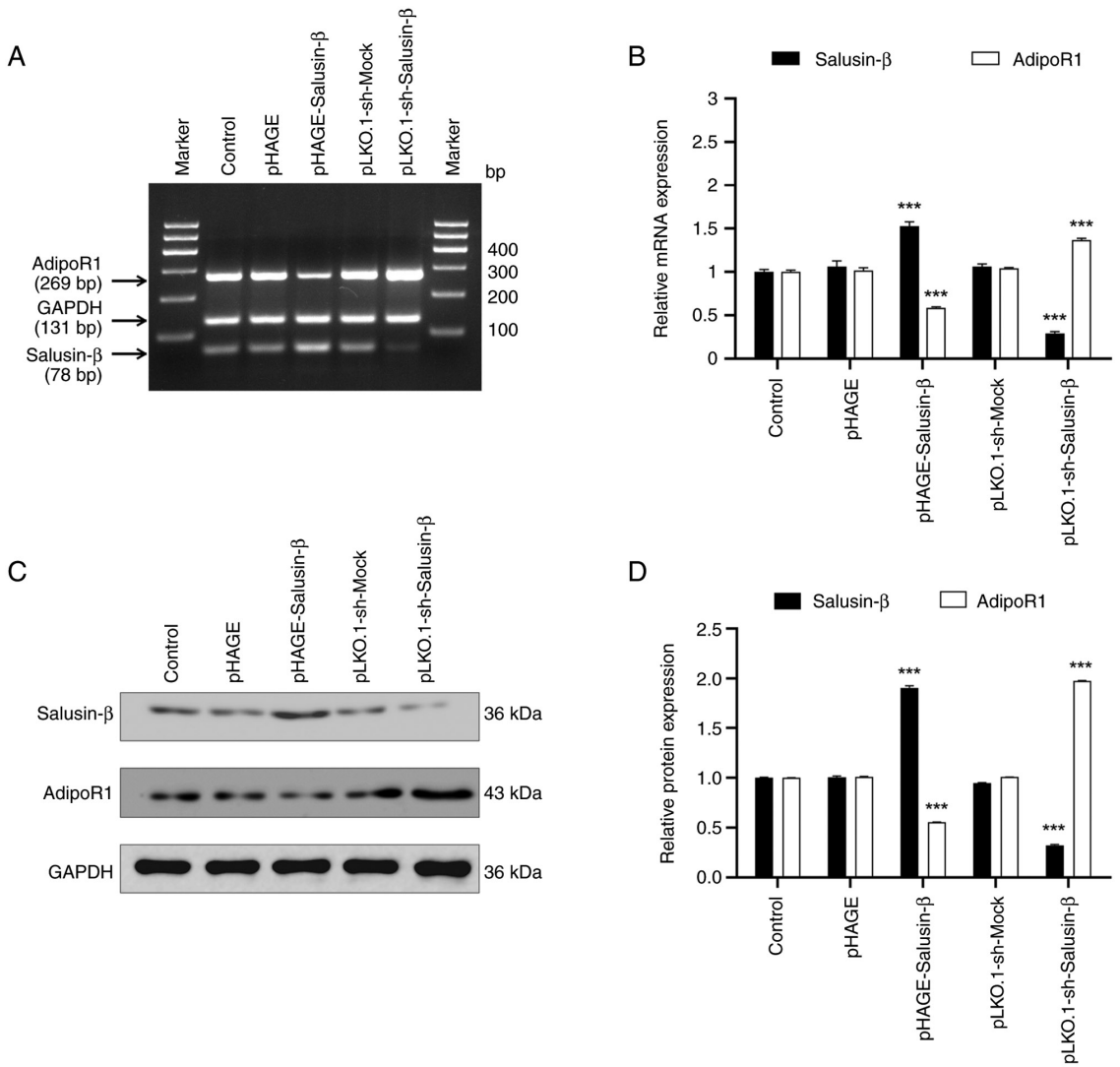

Figure 3. Salusin-β downregulates adipoR1 expression in 293T cells. (A) Electrophoresis of the semi-quantitative PCR products of salusin-β and adipoR1 mRNA from 293T cells transfected with lentivirus for 24 h. The control group was not infected with lentivirus and the experimental groups were transfected with pHAGE, pHAGE-Salusin-β, pLKO.1-sh-Mock, or pLKO.1-sh-Salusin-β lentivirus. (B) Relative mRNA expression levels of salusin-β and adipoR1 in the different groups of transfected 293T cells. (C) Protein expression levels of salusin-β and adipoR1 in 293T cells transfected with lentivirus for 24 h were analyzed by western blotting. (D) Semi-quantification of the protein expression levels of salusin-β and adipoR1. Data are presented as the mean ± standard error of the mean (n=3). ***P<0.001 vs. control group. AdipoR1, adiponectin receptor 1; sh, short hairpin RNA.

was no significant difference in salusin-β mRNA expression between the control group and the groups infected with non-load lentivirus (pHAGE and pLKO.1-sh-Mock groups), which indicated that successful transfection occurred. In the pHAGE-Salusin-β transfection group, increased salusin-β expression led to a decrease in adipoR1 mRNA expression. Conversely, salusin-β shRNA transfection was found to reduce salusin-β mRNA expression whilst increasing adipoR1 mRNA expression. WB analysis confirmed this relationship at the protein expression level (Fig. 3C and D). Specifically, salusin-β overexpression significantly decreased relative adipoR1 protein expression, whilst knocking down salusin-β expression significantly increased adipoR1 protein expression. These findings suggested that salusin-β inhibited adipoR1 mRNA and protein expression in 293T cells.

Salusin-β expression is inversely associated with adipoR1 expression in HepG2 cells. Based on the aforementioned results demonstrating the relationship between salusin-β and adipoR1 expression in 293T cells, HepG2 cells were selected to further investigate this relationship because the liver is closely associated with lipid metabolism and adipoR1 may serve a key role in regulating lipid metabolism (14,15). WB analysis was conducted on transfected HepG2 cells to assess the protein expression levels of salusin-β and adipoR1 (Fig. 4A and B). These results demonstrated that the overexpression of salusin-β in HepG2 cells led to a reduction of adipoR1 protein expression. Furthermore, transfecting HepG2 cells with pLKO.1-sh-Salusin-β_2 decreased the protein expression levels of salusin-β and increased adipoR1 protein expression. These changes in protein expression levels were consistent with those observed in the same corresponding treatment groups of 293T cells, which further confirmed the relationship between salusin-β and adipoR1 expression.

Salusin-β regulates AMPK and ACC phosphorylation and CPT-1A expression through adipoR1 in HepG2 cells. To

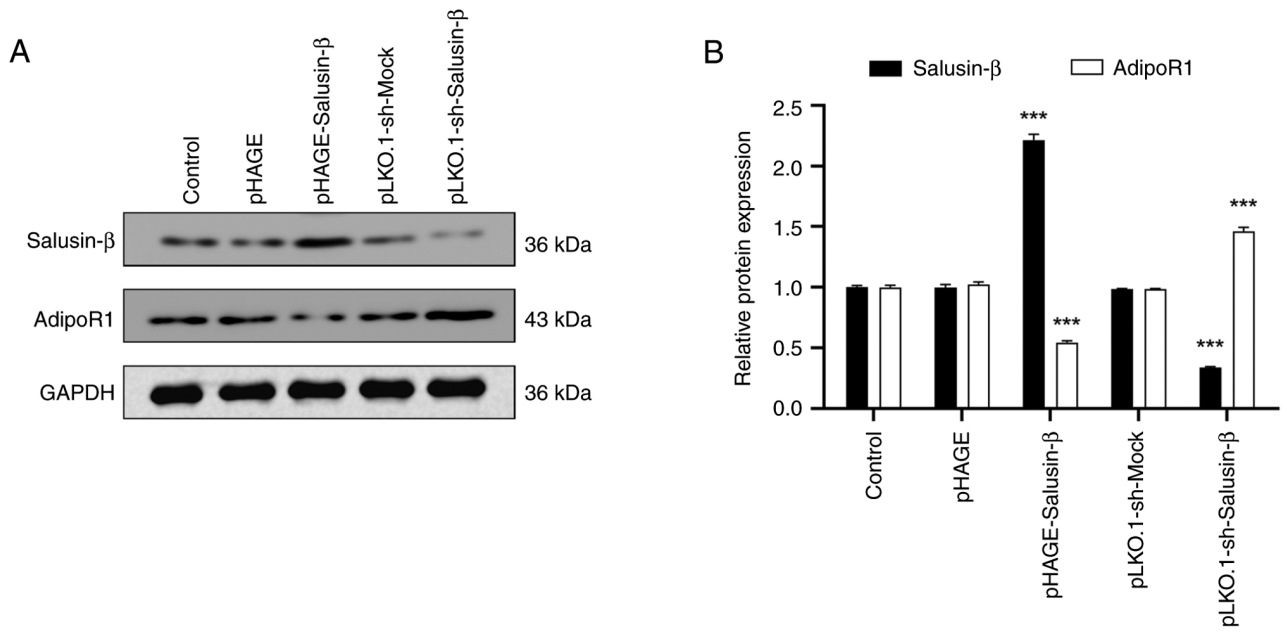

Figure 4. Salusin-β downregulates adipoR1 expression in HepG2 cells. (A) Protein expression levels of salusin-β and adipoR1 in HepG2 cells transfected with lentivirus for 24 h were analyzed by western blotting. (B) Semi-quantification of the protein expression levels of salusin-β and adipoR1. Data are presented as the mean ± standard error of the mean (n=3). ***P<0.001 vs. control group. AdipoR1, adiponectin receptor 1; sh, short hairpin RNA.

investigate the potential regulatory effect of salusin-β on the AMPK/ACC/CPT-1A signaling pathway, the protein levels of p-AMPK and p-ACC, in addition to CPT-1A expression, were examined to assess their modulation by salusin-β. In HepG2 cells, overexpression of salusin-β significantly suppressed AMPK phosphorylation and CPT-1A protein expression, with similar trends observed for p-ACC protein levels (Fig. 5A). However, the western blot analyses showed that there were no marked differences in the total protein expression levels of AMPK and ACC among the treatment groups (Fig. 5A and B). Treatment of HepG2 cells overexpressing salusin-β with the adipoR1 agonist, AdipoRon, led to a significant increase in the protein expression levels of adipoR1 and CPT-1A and increased p-AMPK and p-ACC levels, in contrast to the effects observed for salusin-β overexpression alone. Conversely, transfection of HepG2 cells with sh-Salusin-β_2 resulted in a significant increase in the protein levels of p-AMPK, p-ACC and CPT-1A, all of which were reversed by thapsigargin treatment (Fig. 5B). These findings provide further evidence that salusin-β could specifically modulate the levels of AMPK and ACC phosphorylation, in addition to CPT-1A protein expression, through its interaction with adipoR1.

Salusin-β-mediated downregulation of adipoR1 promotes lipid deposition in HepG2 cells. To further validate the impact of salusin-β-mediated downregulation of adipoR1 on cellular lipid deposition *in vitro*, HepG2 cells transfected with lentiviral vectors were subjected to treatment with FFAs, while a model group induced by FFAs alone and a control group without treatment were also established (Fig. 6A). FFA treatment significantly increased intracellular lipid droplet formation in the model group compared with the control group. In particular, overexpression of salusin-β potentiated the FFA-induced intracellular TG levels and augmented lipid deposition compared with the model group, whereas salusin-β knockdown resulted in reduced TG levels and attenuated intracellular lipid accumulation (Fig. 6B and C). These findings further supported the impact of salusin-β on increasing lipid deposition in HepG2 cells whilst also highlighting its regulatory role in lipid metabolism.

Discussion

Salusin-β is a bioactive peptide that is involved in certain cardiovascular diseases and has been previously associated with abnormal lipid metabolism (16). A previous clinical study reported that serum salusin-β levels are positively associated with TG levels and the TG/HDL ratio in children and adolescents with hypertension (17). A previous *in vitro* study on renal cells reported that salusin-β knockdown reduced lipid droplet formation and cholesterol levels (18). In addition, increased salusin-β expression has been associated with atherosclerosis progression and elevated low-density lipoprotein cholesterol levels in a mouse model (19). Despite these associations, the underlying mechanisms through which salusin-β can modulate lipid metabolism remain elusive. In the present study, the role of salusin-β in lipid metabolism regulation was investigated using both overexpression and knockdown approaches *in vitro*. The 293T cell line was transfected with lentivirus vectors to modulate the expression levels of salusin-β, and then the expression levels of lipid metabolism-related genes were examined. The results demonstrated that salusin-β overexpression suppressed adipoR1 expression in 293T cells, while a decrease in salusin-β levels resulted in increased expression levels of adipoR1. Therefore, in 293T cells, there was a clear inverse relationship between the expression of salusin-β and adipoR1, which indicated a complex interplay between these proteins.

Adiponectin is a key regulator of lipid metabolism that primarily exerts its effects through binding to its receptors,

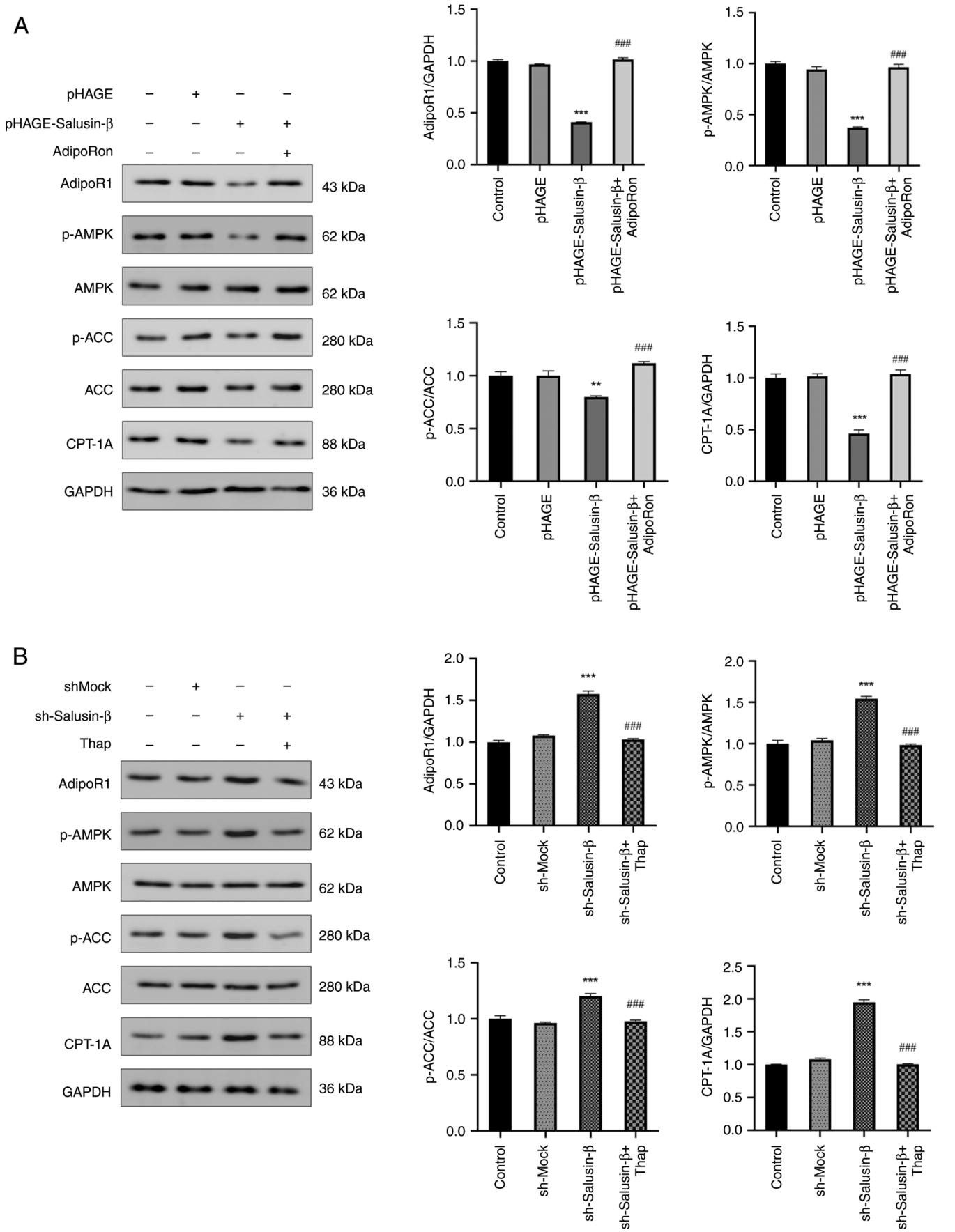

Figure 5. Salusin-β inhibits AMPK and ACC phosphorylation and CPT-1A expression in HepG2 cells. Protein expression levels, analyzed by western blotting, of adipoR1, p-AMPK, AMPK, p-ACC, ACC and CPT-1A in HepG2 cells from each group after 24 h of lentiviral transfection treated with (A) AdipoRon or (B) thap. Data are presented as the mean ± standard error of the mean (n=3). **P<0.01, ***P<0.001 vs. control group. $^{###}$P<0.001 vs. pHAGE-Salusin-β or sh-Salusin-β group. ACC, acetyl-CoA carboxylase; adipoR1, adiponectin receptor 1; AMPK, 5'AMP-dependent protein kinase; CPT-1A, carnitine palmitoyl transferase 1A; p-, phosphorylated; sh, short hairpin RNA; thap, thapsigargin.

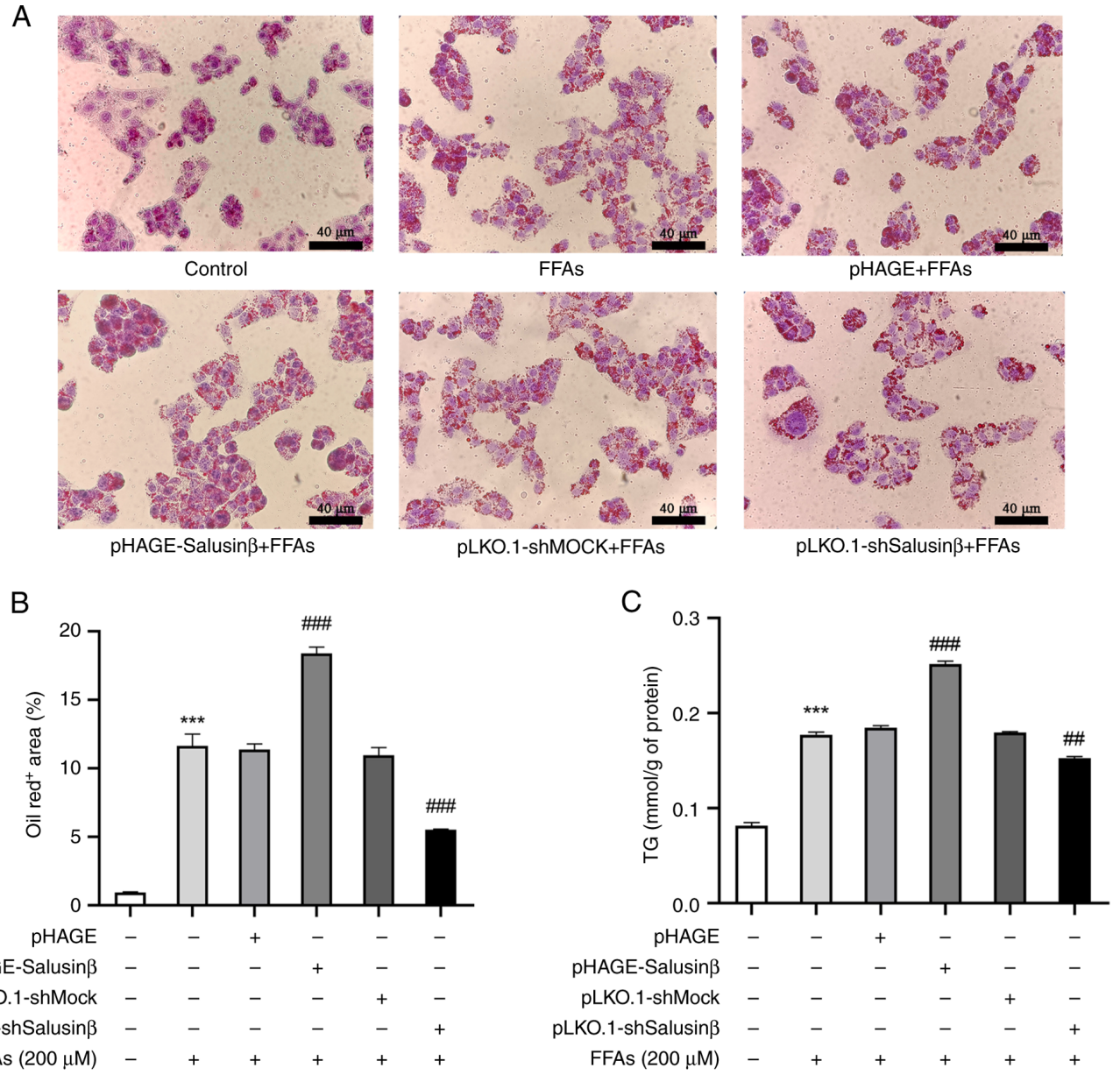

Figure 6. Salusin-β promotes lipid deposition in HepG2 cells. (A) Representative images of Oil Red O staining in HepG2 cells. FFAs induced cellular lipid accumulation in lentivirus-infected cells, characterized by red-stained lipid droplets. Scale bar, 40 μm. (B) Quantification of intracellular lipid content by Oil Red O staining area. (C) Analysis of TG levels in HepG2 cells. Data are presented as the mean ± standard error of the mean (n=3). ***P<0.001 vs. control group. $^{##}$P<0.01, $^{###}$P<0.001 vs. FFAs group. FFAs, free fatty acids; sh, short hairpin RNA; TG, triglyceride.

adipoR1 and adipoR2 (20,21). A number of previous studies have reported that adiponectin, through its interaction with adipoR1, serves a pivotal role in lipid metabolism regulation, whereas salusin-β has been reported to exert contrasting effects (22,23). Considering the critical involvement of the liver in lipid metabolism and the crucial role of hepatocellular lipid deposition in the pathogenesis of fatty liver and related disorders, enhancing hepatocytic lipid metabolism represents a potentially promising therapeutic strategy (14,15). Consequently, HepG2 cells were selected to be the experimental model in the present study. Lentiviral particles harboring the salusin-β-encoding sequence or the shRNA sequence were employed to transfect HepG2 cells. Subsequently, WB was conducted to evaluate changes in adipoR1 protein expression. Consistent with the aforementioned observations in 293T cells, overexpression of salusin-β significantly suppressed adipoR1 expression, whilst salusin-β knockdown had the opposite effect, which further suggested a negative association between salusin-β and adipoR1. However, the precise molecular mechanisms underlying the interaction between salusin-β and adipoR1, in addition to the potential effects on the downstream signaling pathways, warranted further investigation. Further experiments in HepG2 cells were conducted, which also demonstrated consistent alterations in the expression levels of adipoR1 and downstream signaling molecules. In particular, salusin-β overexpression led to the inhibition of AMPK and ACC phosphorylation and the reduction of CPT-1A expression, suggesting its potential involvement in suppressing fatty acid oxidation. Collectively, these results provided evidence to support the pivotal role of salusin-β in modulating lipid

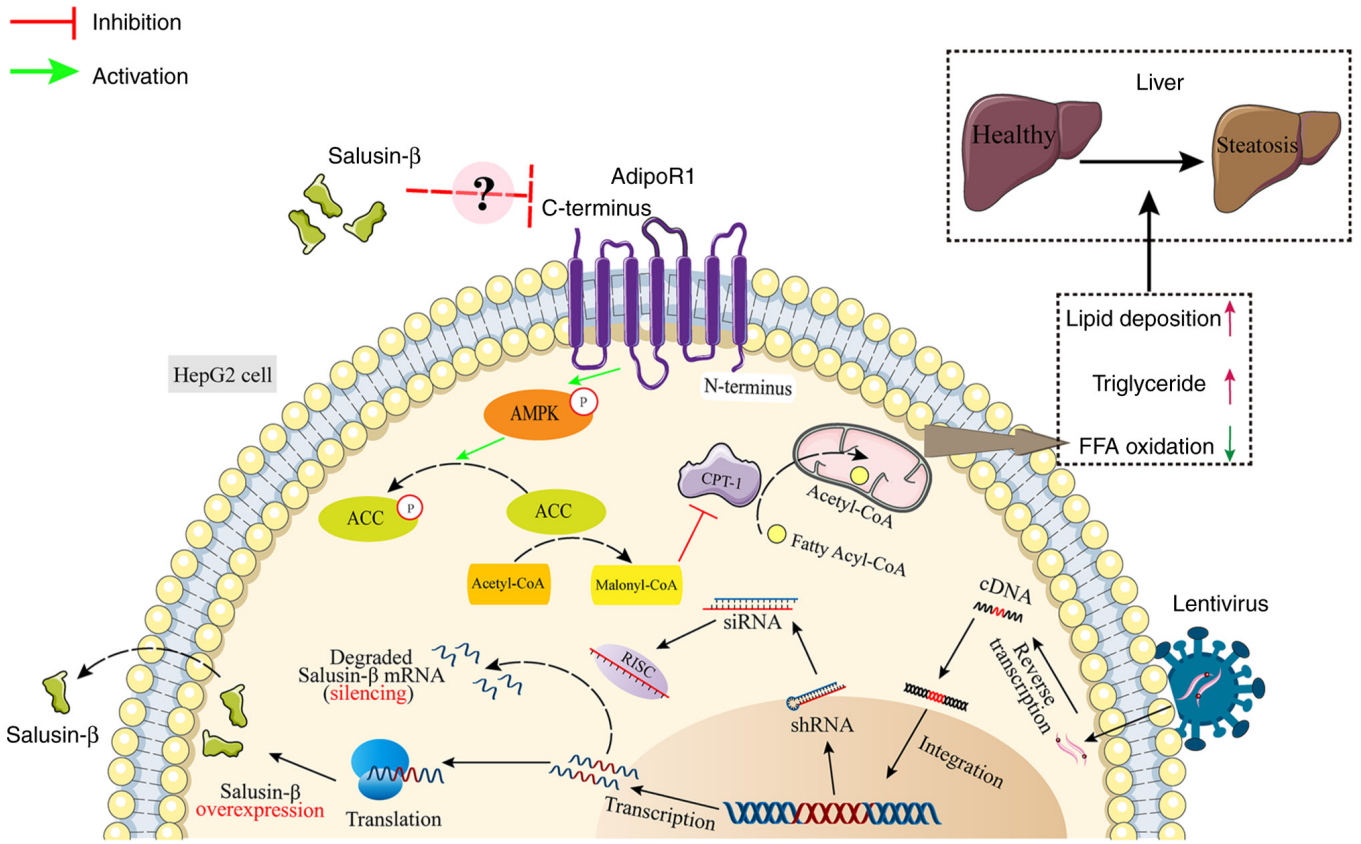

Figure 7. Schematic diagram of the signaling pathway investigated in the present study. Salusin-β decreases adipoR1 expression, which reduces the phosphorylation of AMPK and ACC in cells. ACC promotes the synthesis of Malonyl-CoA, which inhibits CPT-1, reducing the transfer of long-chain fatty acyl-CoA from the cytoplasm to mitochondria, thus inhibiting fatty acid β-oxidation. ACC, acetyl-CoA carboxylase; adipoR1, adiponectin receptor 1; AMPK, 5'AMP-dependent protein kinase; CPT-1, carnitine palmitoyl transferase 1; FFA, free fatty acid; p, phosphorylated; RISC, RNA-induced silencing complex; shRNA, short hairpin RNA; siRNA, small interfering RNA.

metabolism through the adipoR1 signaling pathway in HepG2 cells.

AMPK is a critical regulator of certain metabolic diseases and consists of α, β and γ subunits, with Thr172 on the α subunit acting as the main activation site (24,25). Phosphorylation of Thr172 leads to AMPK activation and the subsequent phosphorylation of ACC at Ser79, resulting in its inactivation and reduced malonyl CoA synthesis (26,27). Malonyl CoA is an intermediate in fat synthesis, and its inhibitory effect on CPT-1 is a key regulatory mechanism for maintaining the balance of fatty acid metabolism, while CPT-1 promotes fatty acid β-oxidation to enhance fat catabolism (28-30). AdipoR1 has been previously associated with the AMPK signaling pathway, with studies reporting its ability to induce Ca^{2+} influx, activate $Ca^{(2+)}$/calmodulin-dependent protein kinase kinase β and upregulate AMPK expression, thereby promoting lipid metabolism (31,32). Conversely, reduced AMPK phosphorylation is associated with lipid accumulation in liver cells (33,34). Notably, salusin-β knockdown in HUVECs has been reported to reverse AMPK and ACC deactivation induced by high glucose (35). Based on these previous findings and those from the present study, specifically the salusin-β-mediated inhibition of adipoR1 expression in HepG2 cells, it was therefore hypothesized that salusin-β may modulate AMPK and ACC phosphorylation, as well as CPT-1A protein levels, through adipoR1, thus influencing lipid metabolism in liver cells. To test this hypothesis, the protein levels of p-AMPK and p-ACC, and CPT-1A expression were examined in different treatment groups of HepG2 cells. WB analysis demonstrated that salusin-β knockdown increased the p-AMPK/AMPK and p-ACC/ACC ratios, in addition to increasing CPT-1A protein expression. By contrast, salusin-β overexpression reduced AMPK and ACC phosphorylation and CPT-1A protein expression. These findings supported the notion that salusin-β can interact with the adipoR1/AMPK signaling pathway, specifically by inhibiting AMPK and ACC phosphorylation and CPT-1A protein expression, by downregulating adipoR1 expression.

According to the data presented in the current study, the inhibitory effect of salusin-β on fatty acid oxidation in HepG2 cells was, at least, partially revealed. Significant changes in CPT-1A protein expression in HepG2 cells were observed after the expression of salusin-β was altered. CPT-1A is a key enzyme in the mitochondrial membrane that is involved in the regulation of fatty acid transport and β-oxidation, which in turn regulates intracellular lipid metabolism (26,28). The results of the present study suggested that by inhibiting CPT-1A, salusin-β may inhibit the ability of hepatocytes to efficiently break down fatty acids by oxidative metabolism, which may lead to lipid accumulation. Therefore, changes in CPT-1A protein expression may be a potential mechanism by which salusin-β inhibits fatty acid oxidation in hepatocytes. In addition, Oil Red O staining was used in

the present study to observe the effect of salusin-β on lipid accumulation in HepG2 cells. The results demonstrated that after salusin-β overexpression, lipid deposition and TG levels were significantly increased in FFA-induced HepG2 cells. This further supported the inhibitory effects of salusin-β on fatty acid metabolism in hepatocytes. In conclusion, based on the results obtained in the present study, it could be suggested that salusin-β may regulate lipid metabolism by acting on the adipoR1/AMPK/ACC/CPT-1A signaling pathway and promoting the deposition of lipids in hepatocytes.

Based on the present experimental findings, a novel hypothesis was proposed (Fig. 7). In HepG2 cells, increased expression of salusin-β leads to the inhibition of adipoR1 expression. This inhibition of adipoR1 then suppresses AMPK activation, which results in reduced p-AMPK levels. Consequently, the activation of ACC by p-AMPK is diminished, which leads to decreased p-ACC and enhanced malonyl CoA synthesis. However, the increased levels of malonyl CoA in turn inhibit the production of CPT-1A, which reduces the entry of long-chain acyl-CoA into the mitochondria and ultimately inhibits fatty acid oxidation.

The present study focused on the regulation of adipoR1 and downstream signaling molecules by modulating salusin-β gene expression. Further research is needed to understand the precise mechanism of the interaction between salusin-β and adipoR1, in addition to its impact on the signaling pathway. A previous study utilized artificial liposomes embedded with endogenous membrane proteins to reveal the direct physical interaction between salusin-β and the ATP synthase β-chain, indicating a potential ligand-receptor binding scenario (36). Salusin-β may potentially activate undiscovered GPCRs (37). This suggests that there may be a physical interaction between salusin-β and adipoR1. However, adipoR1 exhibits a distinct topology compared with other typical GPCRs, with the C-terminal binding to adiponectin located outside the cell whilst the N-terminal binds to adapter proteins inside the cell (9). Additionally, there may be other signaling molecules acting as intermediaries, establishing connections between salusin-β and adipoR1 and influencing the signaling pathway of adipoR1. These specific molecular mechanisms require further investigation. Furthermore, the present study was limited to common lipid metabolism-related molecules. Changes in salusin-β and adipoR1 expression may involve other lipid metabolism pathways. Therefore, further experiments are warranted to elucidate these mechanisms in greater detail.

Acknowledgements

The authors would like to thank Professor Qiuhong Duan (Department of Basic Medicine at the Wuhan Huazhong University of Science and Technology, Wuhan, China) for donating the lentivirus vectors.

Funding

The present study was supported by the ESI Top 1% Discipline Establishment Project for the Hubei University of Chinese Medicine (grant nos. 100702020506 and 100702020518) and the Research Plan Projects of the Hubei Provincial Department of Education (grant no. B2018099).

Availability of data and materials

The datasets used and/or analyzed during the current study are available from the corresponding author on reasonable request.

Authors' contributions

YW, XD and XL proposed the study concepts. AX, LW and HZ designed the study. AX, HZ and MN performed the research. LW, ML and XD provided help and advice with experiments. AX, ML and JP analyzed the data. AX, YW and HZ wrote the manuscript. AX and YW confirm the authenticity of all the raw data. All authors contributed to editorial changes to the manuscript. All authors read and approved the final version of the manuscript.

Ethics approval and consent to participate

Not applicable.

Patient consent for publication

Not applicable.

Competing interests

The authors declare that they have no competing interests.

References

1. Chen MX, Deng BY, Liu ST, Wang ZB and Wang SZ: Salusins: Advance in cardiovascular disease research. J Pharm Pharmacol 75: 363-369, 2023.
2. Shichiri M, Ishimaru S, Ota T, Nishikawa T, Isogai T and Hirata Y: Salusins: Newly identified bioactive peptides with hemodynamic and mitogenic activities. Nat Med 9: 1166-1172, 2003.
3. Xu XL, Zeng Y, Zhao C, He MZ, Wang F and Zhang W: Salusin-β induces smooth muscle cell proliferation by regulating cyclins D1 and E expression through MAPKs signaling pathways. J Cardiovasc Pharmacol 65: 377-385, 2015.
4. Esfahani M, Saidijam M, Najafi R, Goodarzi MT and Movahedian A: The effect of salusin-β on expression of pro- and anti-inflammatory cytokines in human umbilical vein endothelial cells (HUVECs). ARYA Atheroscler 14: 1-10, 2018.
5. Wang Z, Takahashi T, Saito Y, Nagasaki H, Ly NK, Nothacker HP, Reinscheid RK, Yang J, Chang JK, Shichiri M and Civelli O: Salusin beta is a surrogate ligand of the mas-like G protein-coupled receptor MrgA1. Eur J Pharmacol 539: 145-150, 2006.
6. Arkan A, Atukeren P, Ikitimur B, Simsek G, Koksal S, Gelisgen R, Ongen Z and Uzun H: The importance of circulating levels of salusin-α, salusin-β, and heregulin-β1 in atherosclerotic coronary arterial disease. Clin Biochem 87: 19-25, 2021.
7. Aydin S and Aydin S: Salusin-alpha and -beta expression in heart and aorta with and without metabolic syndrome. Biotech Histochem 89: 98-103, 2014.
8. Chen H and Jin G: Downregulation of Salusin-β protects renal tubular epithelial cells against high glucose-induced inflammation, oxidative stress, apoptosis and lipid accumulation via suppressing miR-155-5p. Bioengineered 12: 6155-6165, 2021.
9. Khoramipour K, Chamari K, Hekmatikar AA, Ziyaiyan A, Taherkhani S, Elguindy NM and Bragazzi NL: Adiponectin: Structure, physiological functions, role in diseases, and effects of nutrition. Nutrients 13: 1180, 2021.
10. Wang Q, Liu S, Zhai A, Zhang B and Tian G: AMPK-mediated regulation of lipid metabolism by phosphorylation. Biol Pharm Bull 41: 985-993, 2018.
11. Trudel P, Provost S, Massie B, Chartrand P and Wall L: pGATA: A positive selection vector based on the toxicity of the transcription factor GATA-1 to bacteria. Biotechniques 20: 684-693, 1996.

12. Yu F, Li X, Wang F, Liu Y, Zhai C, Li W, Ma L and Chen W: TLTC, a T5 exonuclease-mediated low-temperature DNA cloning method. Front Bioeng Biotech 11: 1167534, 2023.
13. Zhang Y, Ndzouboukou JB, Lin X, Hou H, Wang F, Yuan L, Gan M, Yao Z, Fu H, Cao J and Fan X: SARS-CoV-2 evolves to reduce but not abolish neutralizing action. J Med Virol 95: e28207, 2023.
14. Sen P, Qadri S, Luukkonen PK, Ragnarsdottir O, McGlinchey A, Jäntti S, Juuti A, Arola J, Schlezinger JJ, Webster TF, *et al*: Exposure to environmental contaminants is associated with altered hepatic lipid metabolism in non-alcoholic fatty liver disease. J Hepatol 76: 283-293, 2022.
15. Alannan M, Fayyad-Kazan H, Trézéguet V and Merched A: Targeting lipid metabolism in liver cancer. Biochemistry 59: 3951-3964, 2020.
16. Wang Y, Wang S, Zhang J, Zhang M, Zhang H, Gong G, Luo M, Wang T and Mao X: Salusin-β is superior to salusin-α as a marker for evaluating coronary atherosclerosis. J Int Med Res 48: 300060520903868, 2020.
17. Kołakowska U, Kuroczycka-Saniutycz E, Wasilewska A and Olański W: Is the serum level of salusin-β associated with hypertension and atherosclerosis in the pediatric population? Pediatr Nephrol 30: 523-531, 2015.
18. Wang WJ, Jiang X, Gao CC and Chen ZW: Salusin-β participates in high glucose-induced HK-2 cell ferroptosis in a *Nrf-2*-dependent manner. Mol Med Rep 24: 674, 2021.
19. Zhou CH, Liu LL, Wu YQ, Song Z and Xing SH: Enhanced expression of salusin-β contributes to progression of atherosclerosis in LDL receptor deficient mice. Can J Physiol Pharmacol 90: 463-471, 2012.
20. Fang H and Judd RL: Adiponectin regulation and function. Compr Physiol 8: 1031-1063, 2018.
21. Pascolutti R, Erlandson SC, Burri DJ, Zheng S and Kruse AC: Mapping and engineering the interaction between adiponectin and T-cadherin. J Biol Chem 295: 2749-2759, 2020.
22. Katsiki N, Mantzoros C and Mikhailidis DP: Adiponectin, lipids and atherosclerosis. Curr Opin Lipidol 28: 347-354, 2017.
23. Niepolski L and Grzegorzewska AE: Salusins and adropin: New peptides potentially involved in lipid metabolism and atherosclerosis. Adv Med Sci 61: 282-287, 2016.
24. Herzig S and Shaw RJ: AMPK: Guardian of metabolism and mitochondrial homeostasis. Nat Rev Mol Cell Biol 19: 121-135, 2018.
25. Cantó C and Auwerx J: AMP-activated protein kinase and its downstream transcriptional pathways. Cell Mol Life Sci 67: 3407-3423, 2010.
26. Fang K, Wu F, Chen G, Dong H, Li J, Zhao Y, Xu L, Zou X and Lu F: Diosgenin ameliorates palmitic acid-induced lipid accumulation via AMPK/ACC/CPT-1A and SREBP-1c/FAS signaling pathways in LO2 cells. BMC Complement Altern Med 19: 255, 2019.
27. Zhang Z, Ni L, Zhang L, Zha D, Hu C, Zhang L, Feng H, Wei X and Wu X: Empagliflozin regulates the AdipoR1/p-AMPK/p-ACC pathway to alleviate lipid deposition in diabetic nephropathy. Diabetes Metab Syndr Obes 14: 227-240, 2021.
28. McGarry JD, Leatherman GF and Foster DW: Carnitine palmitoyltransferase I. The site of inhibition of hepatic fatty acid oxidation by malonyl-CoA. J Biol Chem 253: 4128-4136, 1978.
29. Saggerson D: Malonyl-CoA, a key signaling molecule in mammalian cells. Annu Rev Nutr 28: 253-272, 2008.
30. Dai J, Liang K, Zhao S, Jia W, Liu Y, Wu H, Lv J, Cao C, Chen T, Zhuang S, *et al*: Chemoproteomics reveals baicalin activates hepatic CPT1 to ameliorate diet-induced obesity and hepatic steatosis. Proc Natl Acad Sci USA 115: E5896-E5905, 2018.
31. Liu L, Yao L, Wang S, Chen Z, Han T, Ma P, Jiang L, Yuan C, Li J, Ke D, *et al*: 6-gingerol improves ectopic lipid accumulation, mitochondrial dysfunction, and insulin resistance in skeletal muscle of ageing rats: Dual stimulation of the AMPK/PGC-1α signaling pathway via plasma adiponectin and muscular adipoR1. Mol Nutr Food Res 63: e1800649, 2019.
32. Iwabu M, Yamauchi T, Okada-Iwabu M, Sato K, Nakagawa T, Funata M, Yamaguchi M, Namiki S, Nakayama R, Tabata M, *et al*: Adiponectin and adipoR1 regulate PGC-1alpha and mitochondria by Ca(2+) and AMPK/SIRT1. Nature 464: 1313-1319, 2010.
33. Chen L, Xin FJ, Wang J, Hu J, Zhang YY, Wan S, Cao LS, Lu C, Li P, Yan SF, *et al*: Conserved regulatory elements in AMPK. Nature 498: E8-10, 2013.
34. Long JK, Dai W, Zheng YW and Zhao SP: miR-122 promotes hepatic lipogenesis via inhibiting the LKB1/AMPK pathway by targeting Sirt1 in non-alcoholic fatty liver disease. Mol Med 25: 26, 2019.
35. Zhu X, Zhou Y, Cai W, Sun H and Qiu L: Salusin-β mediates high glucose-induced endothelial injury via disruption of AMPK signaling pathway. Biochem Biophys Res Commun 491: 515-521, 2017.
36. Shichiri M, Nonaka D, Lee LJ and Tanaka K: Identification of the salusin-β receptor using proteoliposomes embedded with endogenous membrane proteins. Sci Rep 8: 17865, 2018.
37. Watanabe T, Nishio K, Kanome T, Matsuyama TA, Koba S, Sakai T, Sato K, Hongo S, Nose K, Ota H, *et al*: Impact of salusin-alpha and -beta on human macrophage foam cell formation and coronary atherosclerosis. Circulation 117: 638-648, 2008.